CHEMISTRY OF MATERIALS
Article

Chem. Mater. **2009,** *21,* 3117–3124 3117
DOI:10.1021/cm900401u

A Platinum(II) Extended Linear Chain Material That Selectively Uptakes Benzene

Steven M. Drew,*,† Lisa I. Smith,‡ Kari A. McGee,‡ and Kent R. Mann‡

† *Department of Chemistry, Carleton College, One North College Street, Northfield, Minnesota 55057, and*
‡ *Department of Chemistry, University of Minnesota, 207 Pleasant Street SE, Minneapolis, Minnesota 55455*

Received February 11, 2009. Revised Manuscript Received May 21, 2009

cis-Bis(isopropyl isocyanide)dicyanoplatinum(II), $Pt^{II}(CN\text{-}i\text{-}C_3H_7)_2(CN)_2$, has been synthesized, and its solid-state characteristics have been investigated. X-ray crystallographic data show that $Pt^{II}(CN\text{-}i\text{-}C_3H_7)_2(CN)_2$ forms an extended linear chain (ELC) material in the solid state that is yellow and luminescent. Exposure of crystalline films of $Pt^{II}(CN\text{-}i\text{-}C_3H_7)_2(CN)_2$ to benzene vapor leads to a solid-state luminescence color change from yellow to blue and a loss of crystallinity. Single-crystal X-ray data obtained for a benzene solvate of $Pt^{II}(CN\text{-}i\text{-}C_3H_7)_2(CN)_2$ suggest that the luminescent blue form observed in the thin film results from a structural rearrangement. In the benzene solvate single crystal the lattice is changed from a staggered to an eclipsed ELC material in which the unit cell has expanded by 20% in volume and contains one benzene molecule for every two $Pt^{II}(CN\text{-}i\text{-}C_3H_7)_2(CN)_2$ molecules. The selectivity, kinetics, and reversibility of this transformation have been studied to determine if crystalline films of $Pt^{II}(CN\text{-}i\text{-}C_3H_7)_2(CN)_2$ would make a useful benzene sensor.

Introduction

Extended linear chain (ELC) materials are composed of one-dimensional molecular arrays of coordination compounds held together by weak metal−metal interactions.[1] These materials have many potential applications as electronic devices, magnetic components, and chemical sensors.[2] Of the ELC materials reported in the literature, those composed of platinum coordination compounds are the most prevalent. Magnus' green salt, $[Pt^{II}(NH_3)_4][Pt^{II}Cl_4]$, was one of the first to be characterized crystallographically and is composed of infinite stacks of alternating square-planar $Pt^{II}(NH_3)_4^{2+}$ dications and $Pt^{II}Cl_4^{2-}$ dianions.[3] Mixed oxidation state platinum ELC materials are also known. For example, Krogmann salts are composed of infinite stacks of square-planar $[Pt^{II/IV}(CN)_4]^{n-}$ anions.[4−6] To date many other families of ELC materials with platinum−platinum interactions have been synthesized and characterized. One family of interest is composed of square-planar Pt(II) complexes with alkyl isocyanide (CNR) and cyanide ligands in the form of either a double salt, $[Pt^{II}(CNR)_4][Pt^{II}(CN)_4]$,[7−10] or its isomeric neutral, $Pt^{II}(CNR)_2(CN)_2$.[11,12] These ELC materials are intensely colored and highly luminescent in the solid state. The term "vapochromic" has been coined to describe the modulation of their solid-state luminescence by various organic vapors. The application of these materials as potential sensors has been the subject of much research.[13−15]

Benzene vapor is a highly regulated volatile organic compound (VOC) due to its known carcinogenic nature. The Occupational Safety and Health Administration (OSHA) has set a legal standard of 1 ppm exposure averaged over an 8 h work day, while the National Institute of Occupational Safety and Health, a division of the Centers for Disease Control, recommends an even lower level of exposure at 0.1 ppm.[16] Monitoring the exposure of workers to VOC hazards such as benzene is technically challenging. The current accepted practices mostly involve the use of an air-sampling pump packed with an absorbent. The absorbent is later extracted and analyzed for VOC's such as benzene using gas chromatography. Research and development of sensors for

(1) Miller, J. S. Extended Linear Chain Compounds; Plenum: New York, 1982; Vols. *1*−*3*.
(2) Bera, J. K.; Dunbar, K. R. *Angew. Chem., Int. Ed.* **2002**, *41*, 4453–4457.
(3) Atoji, M.; Richardson, J. W.; Rundle, R. E. *J. Am. Chem. Soc.* **1957**, *79*, 3017–3020.
(4) Krogmann, K. *Angew. Chem., Int. Ed.* **1969**, *8*, 35–42.
(5) Shriver, D. F. *Inorg. Synth.* **1979**, *19*, 1–18.
(6) Williams, J. M. *Adv. Inorg. Chem. Radiochem.* **1983**, *26*, 235–268.
(7) Daws, C. A.; Exstrom, C. L.; Sowa, J. R.; Mann, K. R. *Chem. Mater.* **1997**, *9*, 363–368.
(8) Exstrom, C. L.; Pomije, M. K.; Mann, K. R. *Chem. Mater.* **1998**, *10*, 942–945.
(9) Exstrom, C. L.; Sowa, J. R.; Daws, C. A.; Janzen, D.; Mann, K. R.; Moore, G. A.; Stewart, F. F. *Chem. Mater.* **1995**, *7*, 15–17.
(10) Buss, C. E.; Anderson, C. E.; Pomije, M. K.; Lutz, C. M.; Britton, D.; Mann, K. R. *J. Am. Chem. Soc.* **1998**, *120*, 7783–7790.
(11) Buss, C. E.; Mann, K. R. *J. Am. Chem. Soc.* **2002**, *124*, 1031–1039.
(12) Dylla, A. G.; Janzen, D. E.; Pomije, M. K.; Mann, K. R. *Organometallics* **2007**, *26*, 6243–6247.
(13) Drew, S. M.; Janzen, D. E.; Buss, C. E.; MacEwan, D. I.; Dublin, K. M.; Mann, K. R. *J. Am. Chem. Soc.* **2001**, *123*, 8414–8415.
(14) Drew, S. M.; Janzen, D. E.; Mann, K. R. *Anal. Chem.* **2002**, *74*, 2547–2555.
(15) Drew, S. M.; Mann, J. E.; Marquardt, B. J.; Mann, K. R. *Sens. Actuators, B* **2004**, *B97*, 307–312.
(16) Centers for Disease Control web site: http://www.cdc.gov/niosh/npg/npgd0049.html.

Published on Web 07/06/2009

Scheme 1

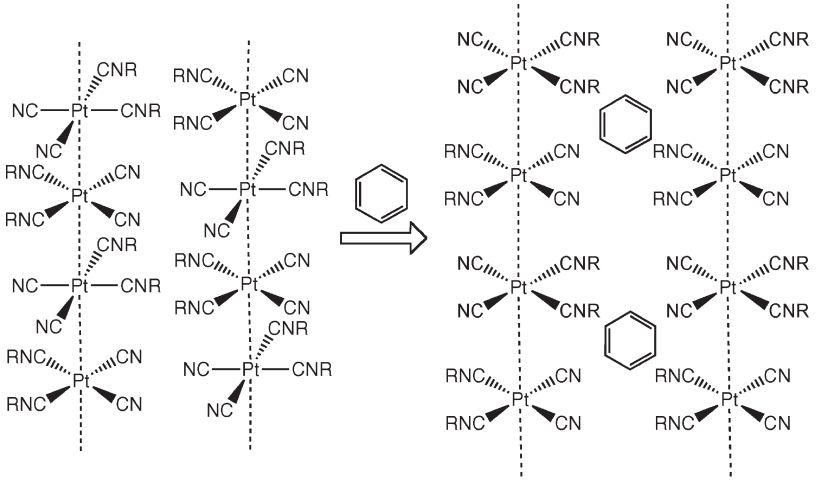

benzene is quite active. Some recently developed sensing devices have been based on diode laser IR absorption spectroscopy,[17] metal oxide semiconductor films,[18−20] and cross-reactive array "electronic nose" sensing.[21−24]

While many good analytical techniques exist for the determination of benzene, their relative expense and inconvenience make the discovery of a material that senses benzene in a reversible manner with high selectivity and sensitivity a desirable goal. In particular, a vapoluminescent material could potentially be useful in developing new benzene sensing techniques. An example of a fluorescent Zn(II) complex immobilized in a polydimethylsiloxane polymer film that responds to benzene vapor has appeared in the literature.[25] In addition, it has been shown that the solid-state luminescence of crystalline materials of the type $Zn^{II}(phen)(aba)_2$, where phen = 1,10-phenanthroline and aba = 4-(dimethylamino)benzoate, can be modulated by benzene, nitrobenzene, and ethanol.[26,27] Our laboratory has chosen this more unified materials approach of designing porous crystalline materials that uptake benzene vapors causing a modulation of solid-state luminescence characteristics, thus eliminating the need for a polymer matrix. Recently, we have shown that benzene sensing is possible with a crystalline Ru(II) polypyridyl tetrakis(bis(3,5-trifluoromethylphenyl)borate) salt via its vapoluminescent response.[6,28] While screening some neutral *cis*-$Pt^{II}(CNR)_2(CN)_2$ ELC materials, we discovered a material that undergoes a considerable change in color upon the formation of a benzene solvate (see Scheme 1). *cis*-Bis(isopropyl isocyanide)dicyanoplatinum(II), $Pt^{II}(CN\text{-}i\text{-}C_3H_7)_2(CN)_2$, has been synthesized, and its solid-state characteristics have been investigated to determine its viability as a useful benzene sensor.

Experimental Section

General Considerations. Isopropyl isocyanide was purchased from Aldrich and used without further purification. Potassium tetracyanoplatinate and platinum(II) acetylacetonate were purchased from Colonial Metals. Spectrophotometric grade benzene was used as a source of benzene vapor. All other solvents used were of ACS reagent grade or better. Attenuated total reflectance (ATR) visible absorption spectra were obtained using an instrument constructed in-house equipped with a cubic zirconia ATR crystal. Exposures to benzene vapor were accomplished by placing several drops of benzene on the edge of the ATR plate and covering with its lid. Thin films of crystalline $Pt^{II}(CN\text{-}i\text{-}C_3H_7)_2(CN)_2$ were cast from acetonitrile solution for all ATR and solid-state luminescence measurements.

***cis*-Bis(isopropyl isocyanide)dicyanoplatinum(II) (1).** $Pt^{II}(CN\text{-}i\text{-}C_3H_7)_2(CN)_2$ was synthesized by literature methods.[11,12] Briefly, the double salt $[Pt^{II}(CN\text{-}i\text{-}C_3H_7)_4][Pt^{II}(CN)_4]$ was synthesized using platinum(II) tetrakis(acetonitrile) triflate,[29,30] isopropyl isocyanide, and tetrabutylammonium tetracyanoplatinate[31] as starting materials according to literature techniques.[7−10] $[Pt^{II}(CN\text{-}i\text{-}C_3H_7)_4][Pt^{II}(CN)_4]$ (0.710 g, 0.922 mmol) was placed in a round-bottom flask under nitrogen and heated to 190 °C in an oil bath for 45 min. During the reaction the color of the solid changed from red

(17) Jeffers, J. D.; Roller, C. B.; Namjou, K.; Evans, M. A.; McSpadden, L.; Grego, J.; McCann, P. J. *Anal. Chem.* **2004**, *76*, 424–432.
(18) Hubalek, J.; Malysz, K.; Prasek, J.; Vilanova, X.; Ivanov, P.; Llobet, E.; Brezmes, J.; Correig, X.; Sverak, Z. *Sens. Actuators, B* **2004**, *101*, 277–283.
(19) Nicoletti, S.; Dori, L.; Cardinali, G. C.; Parisini, A. *Sens. Actuators, B* **1999**, *60*, 90–96.
(20) Zampolli, S.; Betti, P.; Elmi, I.; Dalcanale, E. *Chem. Commun.* **2007**, 2790–2792.
(21) Albert, K. J.; Lewis, N. S.; Schauer, C. L.; Sotzing, G. A.; Stitzel, S. E.; Vaid, T. P.; Walt, D. R. *Chem. Rev.* **2000**, *100*, 2595–2626.
(22) Stitzel, S. E.; Cowen, L. J.; Albert, K. J.; Walt, D. R. *Anal. Chem.* **2001**, *73*, 5266–5271.
(23) Lewis, N. S. *Acc. Chem. Res.* **2004**, *37*, 663–672.
(24) Suslick, K. S.; Bailey, D. P.; Ingison, C. K.; Janzen, M.; Kosal, M. E.; McNamara, W. B.; Rakow, N. A.; Sen, A.; Weaver, J. J.; Wilson, J. B.; Zhang, C.; Nakagaki, S. *Quim. Nova* **2007**, *30*, 677–681.
(25) Pang, J.; Marcotte, E. J.-P.; Seward, C.; Brown, R. S.; Wang, S. *Angew. Chem.* **2001**, *113*, 4166–4169.
(26) Das, S.; Bharadwaj, P. K. *Inorg. Chem.* **2006**, *45*, 5257–5259.
(27) Das, S.; Bharadwaj, P. K. *Cryst. Growth Des.* **2007**, *7*, 1192–1197.
(28) McGee, K. A.; Marquardt, B. J.; Mann, K. R. *Inorg. Chem.* **2008**, *47*, 9143–9145.
(29) Wendt, O. F.; Kaiser, N.-F. K.; Elding, L. I. *J. Chem. Soc., Dalton Trans.* **1997**, 4733–4738.
(30) Kukushkin, V. Y.; Oskarsson, A.; Elding, L. I. *Inorg. Synth.* **1997**, *31*, 279–284.
(31) Mason, W. R.; Gray, H. B. *J. Am. Chem. Soc.* **1968**, *90*, 5721–5729.

to yellow. The final product was dissolved in a minimum amount of methanol and purified by column chromatography (silica gel, methanol) as an orange fluorescent band. A luminescent greenish yellow band remained adsorbed at the head of the silica gel column. Evaporation of the methanol yielded a luminescent yellow solid product in 63% yield (0.447 g, 1.16 mmol). ^{1}H NMR (400 MHz, $CDCl_3$): δ 1.57 (d, $J = 6.6$ Hz, 6 H, CH_3), δ 4.37 (sept, $J = 6.5$ Hz, 1 H, CH). FTIR (ATR, ZnSe crystal): ν_{CNR} 2268, 2251 cm^{-1} (s); ν_{CN} 2156, 2151 cm^{-1} (m). UV−vis (ATR, cubic zirconia crystal): λ_{max} 437 nm. Solid-state luminescence (λ_{ex} 405 nm): λ_{max} 558 nm. HR-ESI-MS: calculated, 385.0918; found, 385.0930 $[M + H]^+$.

Single-Crystal X-ray Diffraction. Crystals of $Pt^{II}(CN\text{-}i\text{-}C_3H_7)_2(CN)_2$ (**1**) were grown by diffusion of ethyl acetate into a saturated solution of $Pt^{II}(CN\text{-}i\text{-}C_3H_7)_2(CN)_2$ in acetonitrile. This yielded yellow luminescent needles after 3 days that were collected and studied. A large amount of thermal motion in the isopropyl groups indicated that they were strongly disordered. Therefore, the C−C bond lengths were restrained to 1.540(1) Å and the angles were fixed to 109.5°. The final full-matrix least-squares refinement converged to R1 = 0.0252 and wR2 = 0.0507 (F^2, all data). Crystals of $Pt^{II}(CN\text{-}i\text{-}C_3H_7)_2(CN)_2 \cdot 0.5C_6H_6$ (**1BNZ**) were obtained from a solution of $Pt^{II}(CN\text{-}i\text{-}C_3H_7)_2(CN)_2$ in acetonitrile layered with benzene. This yielded colorless needles after 1 day that emitted blue light when excited with UV light (λ_{ex} 365 nm). These crystals readily lost solvent, turning yellow. The final full matrix least-squares refinement converged to R1 = 0.0197 and wR2 = 0.0445 (F^2, all data). Crystal and X-ray collection refinement data are summarized in the Supporting Information.

Powder X-ray Diffraction (PXRD). PXRD patterns were collected for samples on aluminum or single-crystal quartz substrates at room temperature between 0 and 60° (2θ) with a Bruker-AXS microdiffractometer equipped with a 2.2 kW sealed Cu X-ray source. Theoretical PXRD patterns were generated from the −100 °C single-crystal data of **1** using Sheltxl software. Samples were prepared either by drop casting of **1** from acetonitrile solution or by adhering lightly ground samples of single-crystal **1** to the sample holder with Dow-Corning high-vacuum grease.

Solid-State Kinetic Measurements and Model Calculations. The solid-state luminescence spectra of crystalline films of **1** were obtained as a function of time using an enclosed chamber that contained saturated benzene vapor. Crystalline films of **1** were obtained by either drop casting or spin casting from acetonitrile solution. Generally, an Ocean Optics spectrometer equipped with a fiber optic fluorescence probe positioned near a crystalline film of **1** was used to collect solid-state luminescence spectra when the film was excited with a UV LED (λ_{max} 405 nm) and exposed to saturated benzene vapor in air. Two methods were used to acquire data to determine if the data acquisition geometry had a significant effect: one in which the spectra were acquired from the back side of a film exposed to benzene vapor and a second method in which the spectra were acquired from the face of the crystalline film in contact with the benzene vapor. Details on the apparatus used to acquire kinetic data are included in the Supporting Information.

Principal component analysis[32,33] (PCA) of the solid-state luminescence spectra as a function of time and the fitting to various solid-state kinetics models were performed using Mathematica. The solid-state kinetic models investigated were Prout−Tompkins, Avrami−Erofeyev, First-Order, and One-Dimension Diffusion.[34] Briefly, the Prout−Tompkins model is an autocatalytic model that includes nucleation and branching.[34] The Prout−Tompkins model generally produces a sigmoidal-shaped curve for fraction converted versus time and also includes an induction time which in essence adjusts the position of the sigmoidal curve along the time axis. The Avrami−Erofeyev model is also a nucleation model that includes processes such as ingestion and coalescence.[34] It also gives a sigmoidal-shaped curve for fraction converted versus time; however, the steepness of the sigmoid can be adjusted by varying the order of the exponential term ($n = 2-4$). First-Order simply refers to an exponential relationship between fraction converted and time that is typical of first-order kinetics. Finally, the One-Dimension Diffusion model treats the conversion of the material as being dependent on the rate of diffusion through the solid. This model has a $t^{1/2}$ time dependence. The solid-state kinetic data showed evidence for an intermediate; therefore, the solid-state kinetic model equations used were derived for a consecutive reaction mechanism of A → B → C. Details of the kinetic equations used to model the observed behavior of the solid-state luminescence spectra as a function of time are included in the Supporting Information.

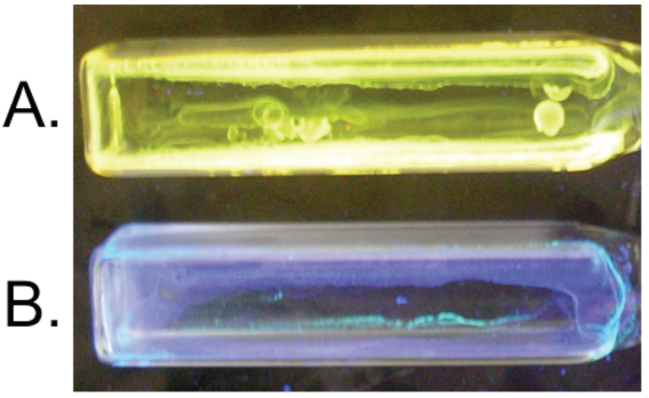

Figure 1. Solid-state luminescence from crystalline films of **1** (λ_{ex} 365 nm) coated on the inside of a cuvette containing (A) air and (B) air saturated with benzene vapor.

Results

A film of $Pt^{II}(CN\text{-}i\text{-}C_3H_7)_2(CN)_2$ (**1**) prepared from acetonitrile solution luminesces bright yellow when excited by UV light. Exposure of this film to benzene vapor causes a dramatic color change. The film becomes colorless and luminesces blue under UV light (see Figure 1) after 1 or 2 h of exposure time, depending on film thickness. PXRD data for a drop cast film of **1** indicates that it is crystalline (see the Supporting Information). Exposure of this crystalline film to benzene gives a putative benzene solvate product that luminesces blue but does not diffract.

The selectivity of crystalline films of **1** for benzene was investigated. Crystalline films were prepared on the inside face of a cuvette from acetonitrile solution. Once the acetonitrile had evaporated and the crystalline film had formed, several drops of a substituted-benzene derivative

(32) Jackson, J. E. A User's Guide to Principal Components; Wiley: New York, 1991.
(33) Beebe, K. R.; Pell, R. J.; Seasholtz, M. B. Chemometrics: A Practical Guide; Wiley: New York, 1998.
(34) Khawam, A.; Flanagan, D. R. *J. Phys. Chem. B* **2006**, *110*, 17315–17328.

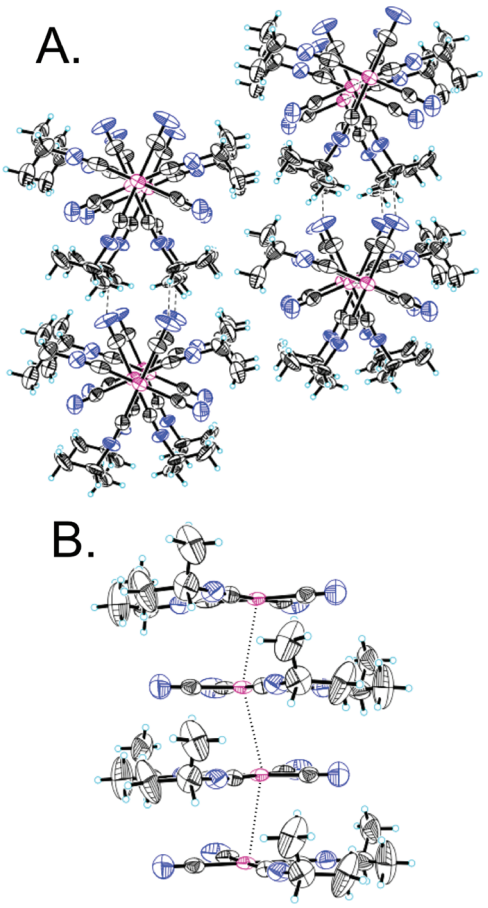

Figure 2. Single-crystal X-ray structure of **1**: (A) view down the *c* axis; (B) view normal to the *c* axis between the *a* and *b* axes. Isopropyl group disorder has been removed for clarity.

were added to the bottom of the cuvette. The cuvette was sealed and left for at least 2 days. Qualitative examination of the films under UV light was used to determine if a reaction had occurred. The substituted-benzene derivatives screened included toluene, *p*-xylene, *m*-xylene, *o*-xylene, mesitylene, chlorobenzene, and hexafluorobenzene. Of the benzene derivatives screened, none showed a significant reaction with crystalline films of **1** after 2 days. Interestingly, a patch of blue luminescence was observed from the film of **1** in the chlorobenzene exposure after 6 days of exposure, but later GC-MS analysis of the chlorobenzene used revealed it was contaminated with benzene at about 0.06 M. Note that when this experiment was repeated with high-purity chlorobenzene, no reaction was observed.

To determine the structural changes that occur in crystalline films of **1** upon exposure to benzene, X-ray-quality crystals were grown in the absence and presence of benzene. As shown in Figure 2, structural data obtained for **1** show that the $Pt^{II}(CN\text{-}i\text{-}C_3H_7)_2(CN)_2$ units form stacks that have Pt−Pt interactions of 3.256 Å. The Pt−C−N bonds are staggered in a view down the *c* axis with symmetry-equivalent Pt−C−N bonds rotated 139° between alternating $Pt^{II}(CN\text{-}i\text{-}C_3H_7)_2(CN)_2$ units[35] in the stack (see Figure 2A).

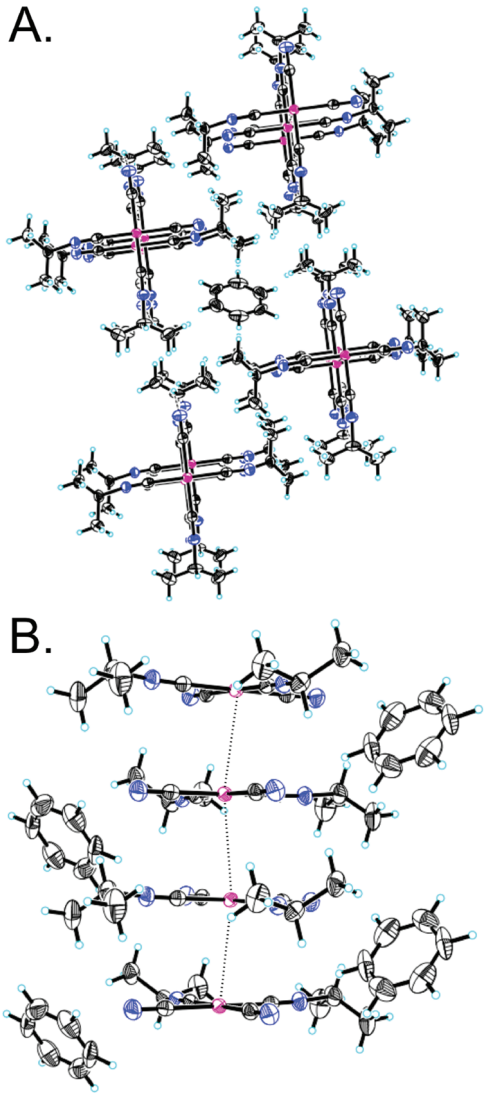

Figure 3. Single-crystal X-ray structure of **(1BNZ)**: (A) view down the *b* axis; (B) view normal to the *b* axis between the *a* and *c* axes.

In addition, the $Pt^{II}(CN\text{-}i\text{-}C_3H_7)_2(CN)_2$ units in **1** are slip-stacked along the *c* axis with a Pt−Pt−Pt bond angle of 160° (see Figure 2B). The crystallographic data obtained for **1** were consistent with previous structures obtained for similar *cis*-$Pt^{II}(CN)_2(CNR)_2$ compounds where R = methyl, ethyl, *tert*-butyl.[36,37] The unit cell volume for **1** fits the expected trend in this series on the basis of the size of R (methyl < ethyl < isopropyl < *tert*-butyl). The structure of $Pt^{II}(CN\text{-}i\text{-}C_3H_7)_2(CN)_2 \cdot 0.5C_6H_6$ (**1BNZ**) also has stacks of $Pt^{II}(CN\text{-}i\text{-}C_3H_7)_2(CN)_2$ units with the addition of benzene solvate molecules that lie on crystallographic inversion centers (see Figure 3), giving **1BNZ** a 2:1 $Pt^{II}(CN\text{-}i\text{-}C_3H_7)_2(CN)_2$ to benzene stoichiometry. The stacking arrangement of $Pt^{II}(CN\text{-}i\text{-}C_3H_7)_2(CN)_2$ units in **1BNZ** differs from that in **1**. Figure 3A clearly shows that the Pt−C−N bonds in **1BNZ** are eclipsed when viewed down the *b* axis, rather than staggered, as seen in **1**. In the case of

(35) Bruno, I. J.; Cole, J. C.; Edgington, P. R.; Kessler, M. K.; Macrae, C. F.; McCabe, P.; Pearson, J.; Taylor, R. *Acta Crystallogr.* **2002**, *B58*, 389–397.

(36) Martellaro, P. J.; Hurst, S. K.; Larson, R.; Abbott, E. H.; Peterson, E. S. *Inorg. Chim. Acta* **2005**, *358*, 3377–3383.

(37) Sun, Y.; Ye, K.; Zhang, H.; Zhang, J.; Zhao, L.; Li, B.; Yang, G.; Yang, B.; Wang, Y.; Lai, S.-W.; Che, C.-M. *Angew. Chem., Int. Ed.* **2006**, *45*, 5610–5613.

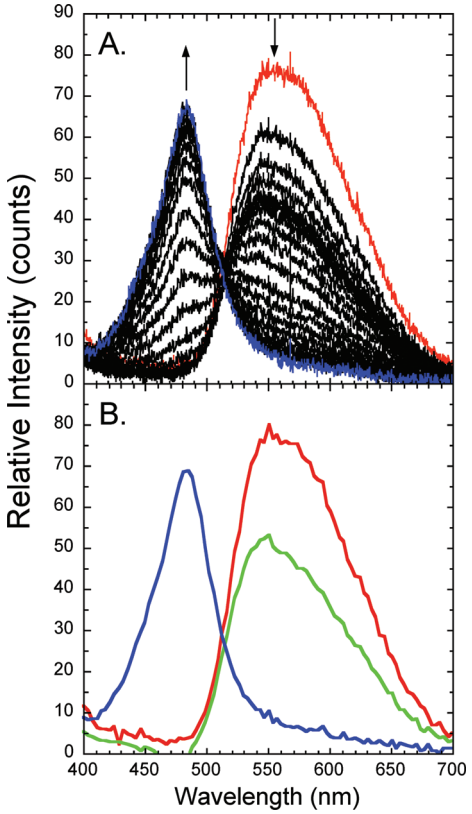

Figure 4. Experimental and regenerated solid-state luminescence spectra of the back side of a crystalline film of **1** in the presence of saturated benzene vapor as a function of time. (A) Experimental spectra: initial spectrum (red) followed by spectra (black) at 4, 6, 8, and 12 min and then from 20 to 150 min in 10 min intervals. The final spectrum (blue) was acquired at 158 min. (B) Regenerated spectra based on a Prout–Tompkins fit of the experimental spectra: (red) species A (**1**); (green) species B (unknown composition); (blue) species C (benzene solvate).

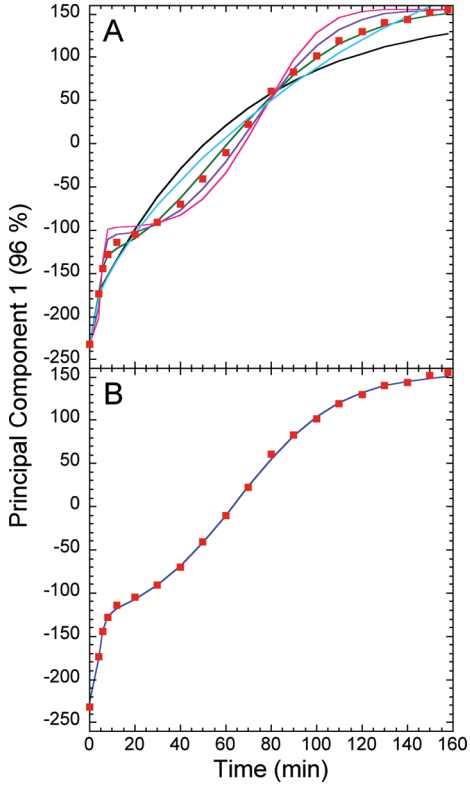

Figure 5. Principal component 1 (red squares) versus time plots including the best fits of solid-state kinetic models for the back side of a crystalline film of **1** in the presence of saturated benzene vapor: (A) Avrami–Erofeyev n = 2 (green), 3 (purple), 4 (pink), First Order (black), and One-Dimension Diffusion (cyan): (B) Prout–Tompkins (blue).

1BNZ equivalent Pt–C–N bonds are rotated by 180° between alternating layers of $Pt^{II}(CN\text{-}i\text{-}C_3H_7)_2(CN)_2$ units.[35] This same packing motif has been observed in the previously reported structure of *cis*-$Pt^{II}(CN)_2(CNC_2H_5)_2$.[36] In addition to bond rotations perpendicular to the *b* axis, the Pt–Pt interaction distance increases to 3.485 Å in **1BNZ**. Interestingly, as shown in Figure 3B the slip-stacked arrangement of the $Pt^{II}(CN\text{-}i\text{-}C_3H_7)_2(CN)_2$ units does not change significantly in **1BNZ** ($\angle$ Pt–Pt–Pt = 161°).

In order to determine the feasibility of using crystalline films of **1** for benzene sensing, the kinetics of benzene uptake were investigated. Solid-state luminescence spectra were acquired for films of **1** in the presence of saturated benzene vapor as a function of time using the two different experimental geometries described in the Supporting Information. The general form of the data did not change significantly with the experimental geometry. Some typical results are shown in Figure 4A. Upon exposure to benzene vapor the initial solid-state luminescence spectrum for **1** (λ_{max} 558 nm) decreases and the luminescence spectrum for a benzene solvate (λ_{max} 484 nm) eventually appears after about 20 min and then increases as a function of time. Careful examination of the spectra from all trials using both experimental geometries revealed that the conversion of **1** to a benzene solvate slowed after about 10 min. As shown in Figure 4A, the spectra are tightly clustered from 12 to 20 min. After the 20 min mark the peak at 558 nm begins to decrease again and the new peak at 484 nm starts to appear. This observation was modeled as a two-step consecutive reaction (A → B → C) that included an intermediate (species B) of unknown structure and composition between those of **1** (species A) and the benzene solvate product (species C).

PCA of the spectral data was used to obtain principal component 1 (PC1), a weighted variable that includes the observed variance in luminescence across the measured spectra. PC1 versus time plots were fit to solid-state kinetic models as described in the Supporting Information. The solid-state kinetic models investigated in this study for A → B → C were Prout–Tompkins, Avrami–Erofeyev (n = 2–4), First-Order, and One-Dimension Diffusion. A typical PC1 versus time plot is shown in Figure 5 along with best fits for the four kinetic models. Table 1 contains a summary of representative kinetic parameters found for all the solid-state kinetic models.

Absorbance spectra measured during the uptake of benzene by **1** were also obtained as shown in Figure 6. These spectra indicate that the wavelength of maximum absorbance shifts to longer wavelength (437 to 458 nm) during the initial exposure to benzene. This is followed by a slower phase that results in the diminution of absorbance at 458 nm and a new absorbance peak growing in at approximately 385 nm. Release of the benzene from the benzene solvate by exposure to the atmosphere gives an absorbance spectrum that does not match the initial

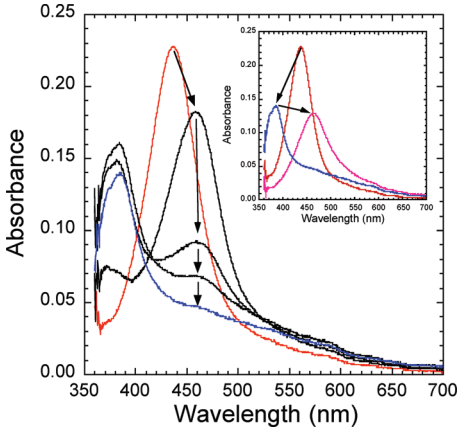

Figure 6. ATR absorbance spectra of benzene uptake and release by a crystalline film of **1**: (main figure) initial spectrum (red) followed by spectra (black) at 5, 36, and 41 min then a final spectrum (blue) at 66 min; (insert) initial spectrum (red, same as main figure), final spectrum after full uptake of benzene (blue, same as main figure), and the spectrum obtained after the release of benzene (pink).

spectrum obtained for a crystalline film of **1** formed from acetonitrile solution (see Figure 6, insert). The wavelength of maximum absorbance in the absence of benzene is now 463 nm. In addition, the absorptivity of the material has been reduced by approximately half.

The reversibility of the uptake of benzene vapor by **1** was investigated by releasing benzene to the atmosphere after a crystalline film of **1** had been converted to its benzene solvate form. The release of benzene was accomplished by removing the benzene-solvated film from the benzene chamber and exposing it to the ambient atmosphere. The luminescence spectrum was observed to red-shift almost immediately back to approximately the same emission wavelength as observed before; however, the intensity of the emission was reduced by at least 50% even after allowing the film to sit in the air for up to 4 h (see Figure S5 in the Supporting Information). Subsequent exposure of this film to benzene did not lead to any significant shift back to the expected spectrum for the benzene solvate even after 9 h of exposure to saturated benzene vapor.

Discussion

Crystalline films of **1** readily uptake benzene vapor from a benzene-saturated atmosphere to produce a non-crystalline benzene solvate film that exhibits an emission spectrum (λ_{max} 484 nm) very similar to that of **1BNZ** (λ_{max} 488 nm), a characterized crystalline form that possesses a 2:1 stoichiometry with benzene. While the PXRD data indicate that long-range order is lost in the benzene solvate film, the similarity in color between the benzene solvate film and **1BNZ** suggests that they are structurally similar, particularly with respect to the Pt−Pt interaction distance. The observed change in color upon exposure of crystalline films of **1** to benzene indicates that the Pt−Pt separation increases as a consequence of this process. This is consistent with the single-crystal X-ray data for **1** and **1BNZ**. The crystallographic data also highlight the extensive changes that likely occur in the crystalline film upon the uptake of benzene. The stacks of $Pt^{II}(CN\text{-}i\text{-}C_3H_7)_2(CN)_2$ units in **1** start in a staggered, slip-stacked conformation along the Pt−Pt interaction axis. Upon exposure of benzene vapor to a crystalline film of **1**, the lattice of individual crystallites likely opens, allowing for the penetration of benzene solvate molecules and leading to the loss of long-range order. This behavior is unlike that of previous vapochromic crystalline materials we have characterized, where benzene enters the lattice through preformed channels.[11,28] However, there is no void space present in **1** (see Table S2 in the Supporting Information) and therefore no preformed channels. When **1** is crystallized in the presence of acetonitrile/benzene, **1BNZ** is obtained. Comparison of **1BNZ** to **1** indicates that there is a 20.2% increase in the unit cell volume that corresponds to the volume of the benzene molecules plus a small volume of new void space (4.1%, see Table S2). Previous PXRD studies of $Pt^{II}(CN\text{-}p\text{-}(C_2H_5)C_6H_4)_2(CN)_2$, a material similar to **1** with the exception that it possesses preformed channels, have shown that when this material is exposed to toluene vapor it expands by approximately 3% and remains crystalline.[11] Therefore, with an increase of 20.2% in unit cell volume when **1BNZ** is compared to **1**, it is not surprising that long-range order is lost when crystalline films of **1** are exposed to benzene vapor.

Perhaps the most striking feature of **1** is its high selectivity for benzene over several other substituted benzene vapors. This was most dramatically and unintentionally demonstrated by the appearance of a patch of benzene solvate after a 6 day exposure of a crystalline film of **1** to chlorobenzene contaminated with benzene. Even though the requirement of a 6 day exposure to 0.06 M benzene indicates a low sensitivity to benzene, the high degree of selectivity is nonetheless impressive.

Our kinetic studies of the uptake of benzene by crystalline films of **1** have provided some additional insight into the transformation that is observed upon the formation of benzene solvate. Brief descriptions of the six solid-state kinetic models studied are in the Experimental Section. Of the models studied, the Prout−Tompkins model most consistently fits the data best. For the data acquired from the back side of a film of **1**, the other fits could be eliminated at the 95% confidence level using the *F*-test (see the Supporting Information). For the data acquired from the front side of a film of **1**, all the other fits could also be eliminated at a 95% confidence level except for the One-Dimension Diffusion model. A comparison of the Prout−Tompkins model results to that of a One-Dimension Diffusion model gives an *F* value of 1.65, indicating a nearly equally good fit for each model (for equally good fits *F* would be unity). However, the spectra and concentration versus time plots calculated using the results of the One-Dimension Diffusion model are inconsistent with the raw data and in some cases are physically impossible (see Figure S4 in the Supporting Information). Therefore, we can eliminate the possibility that a One-Dimension Diffusion model is relevant in describing the solid-state kinetics of the transformation of **1** into a benzene solvate.

Table 1. Solid-State Kinetic Parameter Fit Results

	back side of film fit results[a]					front side of film results[b]				
kinetic model	k_1 (min^{-1})	t_1 (min)	k_2 (min^{-1})	t_2 (min)	β_B	k_1 (min^{-1})	t_1 (min)	k_2 (min^{-1})	t_2 (min)	β_B
Prout−Tompkins	0.73	4.1	0.045	65	−142	0.50	6.1	0.026	39	393
First Order	1.8		0.016		−194	0.38		0.016		338
Avrami−Erofeyev (n = 2)	0.22		0.013		−127	0.11		0.011		177
Avrami−Erofeyev (n = 3)	0.18		0.012		−105	0.092		0.010		134
Avrami−Erofeyev (n = 4)	0.18		0.012		−96.4	0.085		0.010		115
One-Dimension Diffusion	0.00040		0.0068		1060	0.031		0.00037		178

[a] β_A and β_C were set to values of −232.12 and 155.26, respectively, for the fitting processes. [b] β_A and β_C were set to values of 434.92 and −158.96, respectively, for the fitting processes.

Focusing on the Prout−Tompkins model fit parameters listed in Table 1, it appears that the values of the rate constants and induction times do not change significantly with the geometry of data acquisition: i.e., back side or front side of the crystalline film. This apparent lack of significant geometric dependence in the kinetic results allows some additional conclusions to be drawn. First, the spin cast and drip cast crystalline films must not be monolithic but, rather, collections of very small crystallites adsorbed in close proximity to each other on the glass substrate. This allows for benzene vapor to quickly envelop each crystallite of **1** and begin the transformation to benzene solvate. The solid-state luminescence spectrum of the putative intermediate in the transformation has been extracted from the data using the Prout−Tompkins model (see Figure 4B). Note the good agreement between the model-generated spectra in Figure 4B and the experimental spectra shown in Figure 4A. The Prout−Tompkins model effectively generates the initial and final spectra and extracts a physically reasonable spectrum for the intermediate on the basis of the observed "hold up" in the observed spectral conversion. This intermediate spectrum is very similar to the initial spectrum of **1**, except that the emission intensity has decreased. This suggests that the intermediate is a species chemically similar to **1** that has undergone some change in its physical structure or interaction. The absorbance spectra in Figure 6 also provide some insight into the chemical/physical composition of the intermediate. The red shift in absorbance maximum of about 20 nm observed 5 min into a benzene exposure reduces the cross-section of absorbance at the excitation wavelength of 405 nm. Even though there is no observed corresponding 20 nm red shift in the luminescence spectrum of the intermediate, this is nevertheless a viable explanation for the decrease in luminescence intensity as the intermediate is formed. The physical transformation that causes this red shift in absorbance maximum is less clear. One possible explanation is the formation of a layer of adsorbed benzene on the surface of crystallites of **1**. This adlayer may have an effect on the electronics of the Pt−Pt chromophore near the surface of each crystallite. An estimation of light penetration depth can be made by assuming an approximate molar absorptivity for highly colored crystalline **1** of 10^5 M^{-1} cm^{-1}. As seen in the Supporting Information, this leads to a light penetration depth of approximately 200 Å or 20 unit cells for 90% light absorption. Because of the extended electronic structure of platinum ELC materials it is reasonable to hypothesize that the outer 10 or so unit cells of a crystallite that are being probed by the 405 nm excitation light might be affected electronically by an adsorbed layer of benzene.

As an alternative to the hypothesis of an adlayer forming on the crystallites in the film as a physical explanation for the spectroscopically observed intermediate, it is also possible that dispersion in the size of the crystallites leads to the intermediate spectrum. Small, submicrometer-sized crystallites of **1** may be more quickly solvated by benzene than larger ones. In addition, perhaps these small crystallites form a solvated product that lacks the Pt−Pt chromophore needed to observe solid-state luminescence. This would explain the diminution of the intensity of emission from **1** and the lack of emission from the benzene solvate until about 20 min into a benzene vapor exposure (see Figure 4A). After about 20 min the larger crystallites of **1** may start to convert to benzene solvate; however, in this case the crystals are large enough that the inclusion of benzene leads to solvate formation that maintains the Pt−Pt chromophore but induces the loss of long-range order. While we cannot eliminate either of these possibilities, we do however conclude that the presence of the observed intermediate spectrum is best explained as an intermediate physical transformation rather than a chemical species with a distinct intermediate stoichiometry.

Another important observation is that **1** has a slight solubility in benzene (see the Supporting Information). Therefore, the formation of the adsorbed layer of benzene may eventually lead to the formation of a site where **1** is locally converted to benzene solvate starting the conversion of the adlayer intermediate to final product. In other words, the solubility data indicate that there are favorable intermolecular attractions between benzene and **1** that may serve to minimize kinetic barriers in the conversion to the benzene solvate phase. However, the slight solubility of **1** in benzene cannot be used as an explanation for the selectivity of crystalline films of **1** for benzene over other substituted-benzene derivatives. In fact, solubility results indicate a slightly higher solubility of **1** in toluene and mesitylene relative to benzene. The selectivity of crystalline films of **1** for benzene must lie in the absence of a stable solvate phase for adducts such as $Pt^{II}(CN\text{-}i\text{-}C_3H_7)_2(CN)_2 \cdot n(CH_3C_6H_5)$ and $Pt^{II}(CN\text{-}i\text{-}C_3H_7)_2(CN)_2 \cdot n((CH_3)_3C_6H_3)$, since the so-

lubility data imply that there should not be a significant difference in the kinetic barrier.

Reversibility studies indicate that exposure of **1** to benzene to form the benzene solvate cannot be reversed in a facile manner. As shown in Figure S5 (Supporting Information), loss of benzene from the benzene solvate leads to a solid-state luminescence spectrum of lower intensity compared to the initial spectrum of **1**. In addition, attempts to drive the spectrum back to the benzene solvate by re-exposure to benzene failed. These data imply that the crystallinity of films of **1** is key to observing the formation of benzene solvate. It is physically reasonable that these conversions are not easily reversed. The likely rotation of the $Pt^{II}(CN\text{-}i\text{-}C_3H_7)_2(CN)_2$ units from staggered to eclipsed, in addition to the substantial increase in solid-state volume that accompanies the incorporation of benzene into the crystalline lattice of **1**, is a major change indeed. Conversion back to the original crystalline benzene-free form without the aid of solvent molecules is not favorable. However, it is interesting to note that if a drop of acetonitrile is placed on a thin film of **1** that has been "deactivated" by exposure to and removal of benzene, the original spectrum and benzene uptake behavior is again observed.

Conclusion

The neutral platinum(II) ELC material $Pt^{II}(CN\text{-}i\text{-}C_3H_7)_2(CN)_2$ (**1**) has been synthesized and characterized. Exposure of crystalline thin films of **1** to benzene leads to the highly selective uptake of benzene to form a benzene solvate. Even though long-range order is lost in the benzene solvate film, solid-state luminescence data indicate that it is similar in structure to a characterized single-crystal benzene solvate: $Pt^{II}(CN\text{-}i\text{-}C_3H_7)_2(CN)_2\cdot 0.5C_6H_6$ (**1BNZ**). X-ray crystallographic data for **1** and **1BNZ** highlight the substantial structural changes that likely accompany the uptake of benzene in thin films of **1**. The Prout−Tompkins model was found to be the best choice for modeling the solid-state kinetic behavior of this system. Kinetic studies of the benzene uptake process provided evidence for the presence of an intermediate species. Spectroscopic and kinetic analysis resulted in the conclusion that the intermediate was best modeled as a physical transformation of **1** due either to the adsorption of benzene or to the differential solvation behavior of small versus large crystallites. The uptake selectivity of crystalline films of **1** for benzene over substituted-benzene derivatives was best explained as a lack of stability in potential adducts that could be formed. While the uptake of benzene by **1** was found to be slow, was of low sensitivity, and was not reversible due to crystalline degradation, other derivatives of these types of materials may be found that could form the basis of a practical benzene-sensing device.

Acknowledgment. Sabbatical support for S.M.D. was provided by Carleton College and an Eugster Faculty Development Grant. Research funds were provided by the Center for Process Analytical Chemistry (CPAC) at the University of Washington and the Initiative for Renewable Energy and the Environment at the University of Minnesota through grants to K.R.M. We acknowledge Dr. Victor G. Young, Jr., and the University of Minnesota X-ray Crystallographic Laboratory. Parts of this work were carried out in the Institute of Technology Characterization Facility, University of Minnesota, which receives partial support from the NSF through the NNIN program.

Supporting Information Available: Text, tables, and figures giving PXRD data, crystal structure refinement details, solid-state kinetic measurements and model calculations, reversibility studies, estimations of penetration depth, and relative solubility measurements and CIF files giving X-ray crystallographic data. This material is available free of charge via the Internet at http://pubs.acs.org.